Numerical investigation of nonlinear oscillations of gas bubbles in liquids*

Werner Lauterborn

Drittes Physikalisches Institut, Universität Göttingen, D-34 Göttingen, West Germany
(Received 28 December 1973; revised 27 August 1974)

Forced oscillations of a spherical gas bubble in an incompressible, viscous liquid (water) are calculated numerically. The information gathered is mainly displayed in the form of frequency response curves of the steady-state solutions showing the harmonics, subharmonics, and ultraharmonics. Bubbles oscillating ultraharmonically at frequencies below the main resonance may emit half the driving frequency. This fact gives rise to a new explanation for the occurrence of the first subharmonic in the spectrum of the cavitation noise in ultrasonic cavitation.
Subject Classification: [43]30.70, [43]30.75.

INTRODUCTION

Bubble dynamics is one of the basic problems in cavitation. Its theoretical investigation is a rather involved problem. Therefore, various bubble models have been developed (see the first monographs on cavitation[1–3]) which are simple enough to be evaluated either analytically or numerically. Because of the highly nonlinear nature of even the simplest models, analytical investigations have been found to be extremely difficult[4] unless further approximations are made.

The development of fast digital computers has made possible a thorough numerical investigation of these models. But as an enormous amount of computer time is needed, so far only some aspects of bubble dynamics have been calculated.[1–3] This paper tries to give a more thorough survey of the basic properties of a special bubble model by extensive use of fast digital computers. The response of a bubble to a sound field is calculated evaluating mainly the steady-state solutions (radius–time curves and spectra). Frequency response curves are given for different pressure amplitudes of the sound field as well as for different bubble radii. For sufficiently high values of the pressure amplitude, however, no steady-state solutions may be obtained within a reasonable time because of catastrophic excursions of the oscillation amplitude. Thus bubble behavior at higher sound pressure amplitudes can not be given in terms of response curves based on steady-state solutions. Nevertheless, this region seems to be of interest because of its supposed relation to the onset of cavitation.

Special attention is given to those oscillations yielding an emission at half the driving frequency because the occurrence of this spectral line in the spectrum of cavitation noise is a peculiar feature of acoustic cavitation up to now not fully understood. It has first been observed by Esche[5] and since then attracted the attention of many authors.[4,6–15] The first explanation was attempted by Güth.[4] He pointed out that a bubble driven at twice its resonance frequency may exhibit oscillations at its resonance frequency, thus being the source of the observed subharmonic signal in the cavitation noise spectra. This view is now generally accepted, but the calculated spectra of bubble oscillations given below reveal that also bubbles driven below resonance may exhibit strong subharmonic components in the spectrum, especially the ultraharmonics of order $n/2$, $n = 3, 5, \ldots$. Thus in a real cavitation bubble field, bubbles of greatly different sizes and even when driven below resonance may add to the subharmonic signal. Details are discussed below.

I. THE BUBBLE MODEL

A sketch of the bubble model used is given in Fig. 1. showing the physical parameters defining the model.

The bubble is supposed to remain spherical throughout its motion (having a momentary radius R and a radius at rest R_n) and to be surrounded by an infinitely extended incompressible liquid of density ρ. Thus shape stability questions and damping of the bubble due to sound radiation are not considered. Also thermal problems and problems of gas diffusion through the bubble wall are neglected. Included in the model are the effects of surface tension σ and shear viscosity μ. The viscosity is taken to be constant, that means the

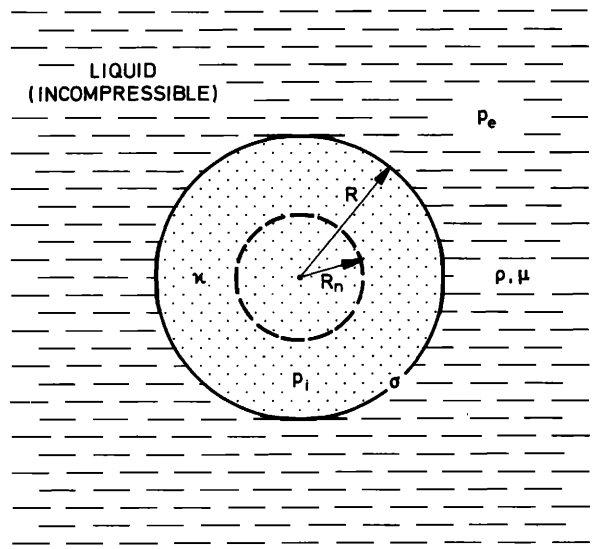

FIG. 1. The bubble model used showing parameters and notation: spherical bubble in an infinitely extended incompressible viscous liquid. R_n is the radius of the bubble at rest, R momentary radius; p_i, the internal pressure (sum of gas and vapor pressure; p_e, the external pressure [sum of static pressure p_{stat} and arbitrary varying pressure $p(t)$]; ρ, the density; μ, the viscosity; σ, the surface tension of the liquid; and κ, the polytropic exponent of the gas inside the bubble.

model is restricted to bubbles in Newtonian liquids. The bubble will contain some gas and vapor of total pressure p_i. It is assumed that the vapor pressure p_v remains constant during the motion. The gas in the bubble is compressed according to a polytropic gas law, with the polytropic exponent κ remaining constant during the motion. The external pressure $p_e(t)$ is the sum of a static pressure p_{stat} (being the sum of the atmospheric pressure and the hydrostatic pressure) and an arbitrary, but not too fast varying pressure $p(t)$ (for instance an applied sound field). In the case of water at 20 °C (as considered below) p_v will be small and, as taken to be constant, will change the value of p_{stat} only slightly.

When this bubble model is given a mathematical form, the following nonlinear ordinary differential equation of second order is obtained[16–19]:

$$\rho R\ddot{R} + \tfrac{3}{2}\rho\dot{R}^2 = p_g\left(\frac{R_n}{R}\right)^{3\kappa} + p_v - p_{\text{stat}} - \frac{2\sigma}{R} - \frac{4\mu}{R}\dot{R} - p(t), \quad (1)$$

with

$$p_g = \frac{2\sigma}{R_n} + p_{\text{stat}} - p_v\,, \quad (2)$$

where a dot denotes a derivative with respect to time. This model is suggested to be called the RPNNP-bubble model after Rayleigh,[16] Plesset,[17] Noltingk and Neppiras,[18] and Poritsky[19] who contributed to its mathematical formulation. In the numerical calculations reported here $p(t)$ was taken as sinusoidal of the form

$$p(t) = -p_A \sin\omega t\,, \quad (3)$$

p_A being the sound pressure amplitude and ω the angular frequency of the sound field. The negative sign in Eq. (3) is adopted to start with tension at $t = 0$. As $p(t)$ must be constant at the bubble surface, the wavelength of the sound wave must be large compared to the bubble radius. This holds true for frequencies up to far above the linear resonance frequency ν_0 of the bubble given by

$$\nu_0 = \frac{1}{2\pi R_n\sqrt{\rho}}\left[3\kappa\left(p_{\text{stat}} + \frac{2\sigma}{R_n} - p_v\right) - \frac{2\sigma}{R_n} - \frac{4\mu^2}{\rho R_n^2}\right]^{1/2}, \quad (4)$$

so that response curves in a broad surrounding of the main resonance do not suffer from this restriction. Indeed, when this condition is not fulfilled, the bubble will no longer remain spherical upon excitation, and the above model [Eqs. (1)–(3)] will fail to describe bubble behavior.

II. RESULTS

When solving the differential Eq. (1) on a digital computer, it turned out that the number of parameters involved was too big to be altered independently to get almost all interesting cases. But not all possible variations of the parameters will be meaningful. For instance, the set of parameters (ρ, σ, μ) is associated with the liquid and not all combinations [in fact only a very limited part of the (ρ, σ, μ) space] will correspond to real liquids. Besides, as water is by far the most interesting liquid, the investigation is restricted to bubbles in water, more precisely to bubbles in water at 20 °C ($\rho = 0.998$ g cm^{-3}, $\sigma = 72.5$ dyn cm^{-1}, $\mu = 0.01$ g cm^{-1} sec^{-1}, $p_v = 0.0233$ bar). As a further restriction the static pressure is always given the value $p_{\text{stat}} = 1$ bar and the polytropic exponent the value $\kappa = 1.33$.

Forced oscillations are calculated with these values for different bubble radii. The parameters varied are the bubble radius at rest R_n, the sound pressure amplitude p_A, and the sound field frequency $\nu = \omega/2\pi$. There will be a dependence of the solutions on the initial conditions. This important question is touched only slightly because of computer time limitations. Most calculations were done starting with the initial conditions

$$R(t=0) = R_n \text{ and } \dot{R}(t=0) = 0.$$

After a certain number of oscillations (for pressure amplitudes p_A not too high), the oscillations $R(t)$ become periodic, the period T_R being an integral multiple of the sound field period $T = 1/\nu$:

$$T_R = mT, \quad m = 1, 2, 3\ldots .$$

T_R can also be an integral multiple of a so-called free oscillation of the gas bubble with a period T_f

$$T_R = nT_f, \quad n = 1, 2, 3, \ldots .$$

As T_f strongly depends on the "amplitude" (for a definition of the amplitude, see below) of the oscillation, it is clear, that the introduction of T_f may not be meaningful and even impossible as it turns out to be the case for sufficiently strong oscillations (being nevertheless steady-state oscillations).

The oscillations show special features when the frequency ν of the sound field and the amplitude p_A are altered. For not too high values of p_A resonances may be observed which can be associated with the numbers n and m. The expression n/m is then called the order of the resonance. The case $m = 1$, $n = 2, 3, \ldots$ denotes the well known harmonics, the resonances when $n = 1$ and $m = 2, 3, \ldots$ are called subharmonics of order $\frac{1}{2}$, $\frac{1}{3}$, ... (often for simplicity called first subharmonic, second subharmonic, ...). The resonances when $n = 2, 3, \ldots$ and $m = 2, 3, \ldots$ are called ultraharmonics. As was noted above, the introduction of T_f may be impossible. This occurs when the classification of to what resonance the observed steady-state oscillation may belong cannot be concluded from the parameter values p_A and ν. Thus a more general notation will be one distinguishing only between $m = 1$ (called harmonic responses) and $m = 2, 3, \ldots$ (called subharmonic responses).

Figure 2 shows an example of a steady-state solution of Eq. (1) for a specific parameter set as plotted automatically along with additional tables on a line printer. The upper curve is the driving sound pressure, the curve in the middle is the resulting steady-state bubble oscillation (radius time curve) and the lines below are the first few spectral lines of the amplitude spectrum of the (periodic) oscillation. The spectrum is plotted in such a way that the driving frequency is always located at 1 on the abscissa. The example shows an ultraharmonic of order n/m with $n = 5$ and $m = 2$ (the M in Fig. 2 is this same m). It has a rather strong component at half the driving frequency (and its odd har-

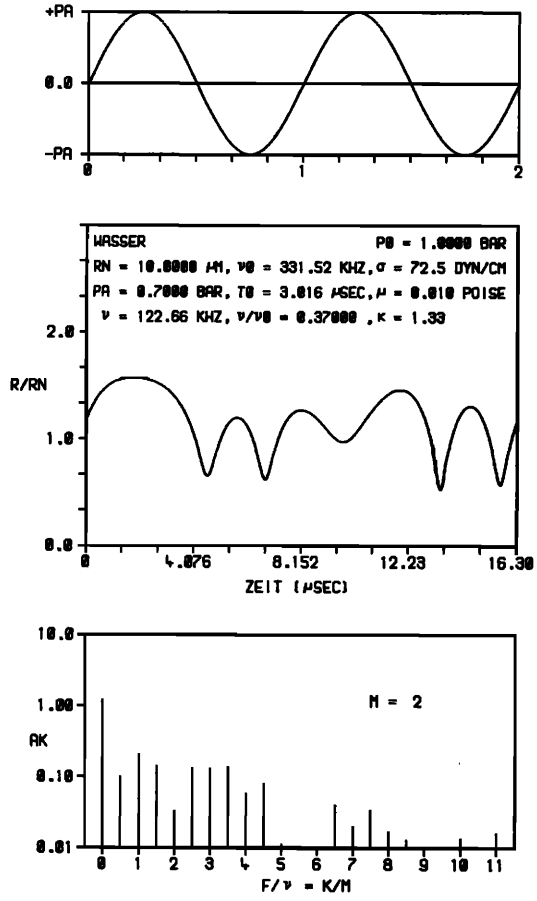

FIG. 2. Example of the computer output for a given parameter set as noted in the second frame ($P\phi = p_{stat}$). The steady-state oscillation (second frame) is an ultraharmonic of order $\frac{5}{2}$. It is periodic with two cycles of the driving sound field (upper frame). The amplitude spectrum of the bubble wall motion is given in the lower frame. AK are the coefficients in the Fourier expansion; F is the frequency in the spectrum; ν, the frequency of the driving sound field; K, the number of the harmonic in the spectrum; and M, the number of the periods of the driving sound field after which the bubble repeats its cycle again (being the same as the denominator of the order of the resonance).

monics), whereas being driven far below the main resonance. The implications of this fact will be discussed below.

Many of such data sheets as shown in Fig. 2 were plotted to gain an insight into the behavior of bubbles in sound fields.

A. General behavior of the frequency response curves

Frequency response curves are calculated for three different bubble radii, i.e., $R_n = 10$ μm (Fig. 3), $R_n = 1$ μm (Fig. 4), and $R_n = 0.1$ μm (Fig. 5). The bubble size of $R_n = 10$ μm is included in the investigation although it is known that for a bubble of this size in water the damping due to viscosity is only slight and that heat conduction and sound radiation will be of major importance. Thus it cannot be expected that the bubble model [Eq. (1)] will yield a quantitative agreement with some sort of measurements. But this model may serve as a standard basis (*the* basis) and background to which all measurements (and also calculations) can be related. Insofar this model is fundamental though not at all complete.

The three cases considered correspond to systems of slight ($R_n = 10$ μm), moderate ($R_n = 1$ μm), and heavy ($R_n = 0.1$ μm) damping. The normalized "amplitude" $(R_{max} - R_n)/R_n$ (R_{max} is the maximum radius of the bubble during its steady-state oscillation) is plotted as a function of the normalized frequency ν/ν_0, where ν is the frequency of the applied sound field and ν_0 the linear resonance frequency of the bubble according to Eq. (4). The range for ν/ν_0 was chosen from about 0.15 to 2.5. Certain other ranges, for instance near $\nu/\nu_0 = 3$, will be discussed in separate sections. The range of pressure amplitudes p_A was chosen individually for each of the three radii R_n considered, up to 0.8 bar for $R_n = 10$ μm, up to 1.6 bar at $R_n = 1$ μm and up to 17 bar at $R_n = 0.1$ μm. These limits were set by the fact, that at or somewhat above these values in certain regions of ν/ν_0 no steady-state solutions could be obtained or extremely long computer time was needed to get the solutions.

The resonance curves (Figs. 3–5) show a lot of special features like harmonics, subharmonics, and ultraharmonics (especially Fig. 3, the slightly damped system), further jumps, frequency shifts of resonances, and thresholds for subharmonics and ultraharmonics. At small bubble radii (Figs. 4 and 5) the resonances are strongly damped and even totally suppressed. This holds true especially for the subharmonics and ultraharmonics. They only occur above a threshold value of the sound pressure amplitude p_A. These threshold are raised to high values when the bubble radius is lowered.

Above a certain value of p_A the amplitude of the stationary solution grows steadily when the frequency ν of the sound field is lowered. This not only holds true for small bubbles (Fig. 5, $R_n = 0.1$ μm), but also big bubbles (Fig. 3, $R_n = 10$ μm). But because of the slow convergence towards stationarity and perhaps no convergence at all, only a few solutions could be obtained in this region of the parameters p_A and ν/ν_0 for $R_n = 10$ μm. The growing of the amplitude of the oscillation at sufficiently high pressure amplitudes towards lower frequencies is a consequence of the fact that a bubble in water can not withstand arbitrary high static tension but will grow infinitely beyond a static tension threshold called the Blake threshold (see Flynn[1]), given by

$$p_B = p_{stat} - p_v + \frac{4\sigma}{3\sqrt{3}R_n}\left[1 + (p_{stat} - p_v)\frac{R_n}{2\sigma}\right]^{-1/2}, \qquad (5)$$

when isothermal expansion is assumed. The values are $p_B = 0.997$ bar for $R_n = 10$ μm, $p_B = 1.408$ bar for $R_n = 1$ μm and $p_B = 6.379$ bar for $R_n = 0.1$ μm. They fit well into the behavior of the resonance curves at low frequencies.

In the following sections we will have a closer look at the different resonances and features of bubble oscillations.

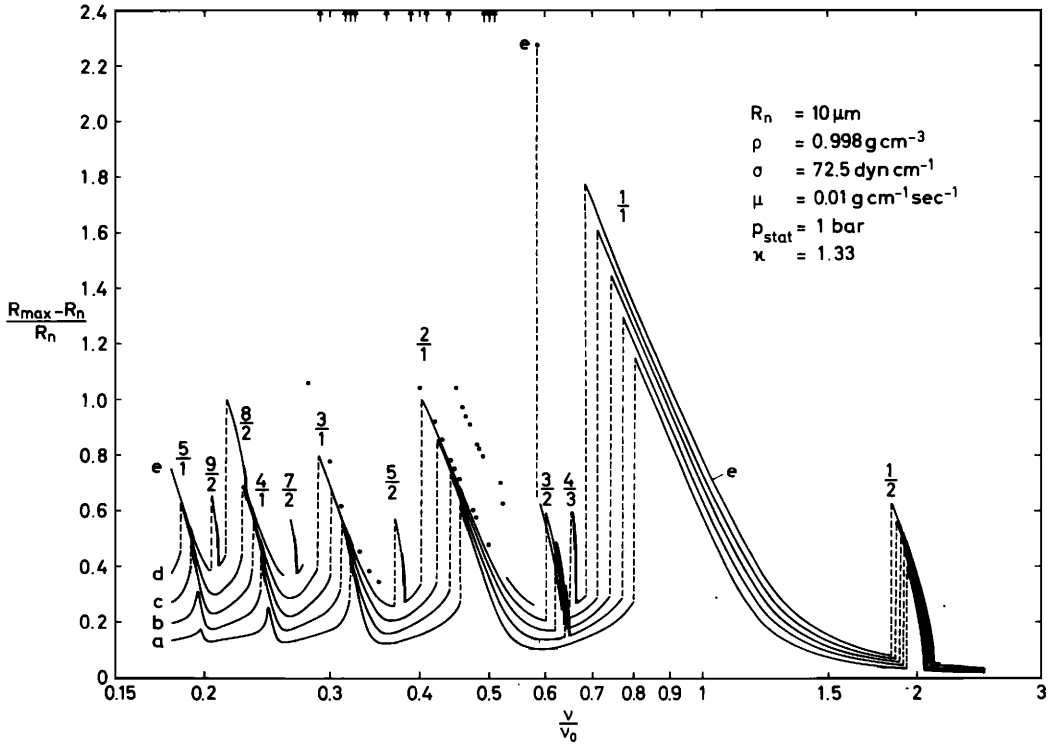

FIG. 3. Frequency response curves for a bubble in water with a radius at rest of $R_n = 10\ \mu m$ for different sound pressure amplitudes p_A of (a) 0.4, (b) 0.5, (c) 0.6, (d) 0.7, and (e) 0.8 bar. The numbers occurring above the peaks of the curves are the orders of the resonances. The dots and the arrows belong to curve (e). The arrows indicate that the corresponding stationary solution is out of the range of the diagram or that no stationary solution could be found. In this case the amplitude values were also very high oscillating around some value outside the diagram.

B. Main resonance

The resonance in the region around $\nu/\nu_0 = 1$ is the main resonance. It leans over towards lower frequencies (indicating a soft spring on the average) and jumping phenomena occur at sufficiently high pressure amplitudes. The location of the jump depends on the initial conditions or the direction of frequency alteration. When, as in Figs. 3–5, the initial conditions $R(t=0) = R_n$ and $R(t=0) = 0$ are used, the lower stable branch is reached corresponding to the curve the bubble would follow when the frequency is increased from sufficiently low values. To obtain the upper stable branch, the calculations were done in the following way.

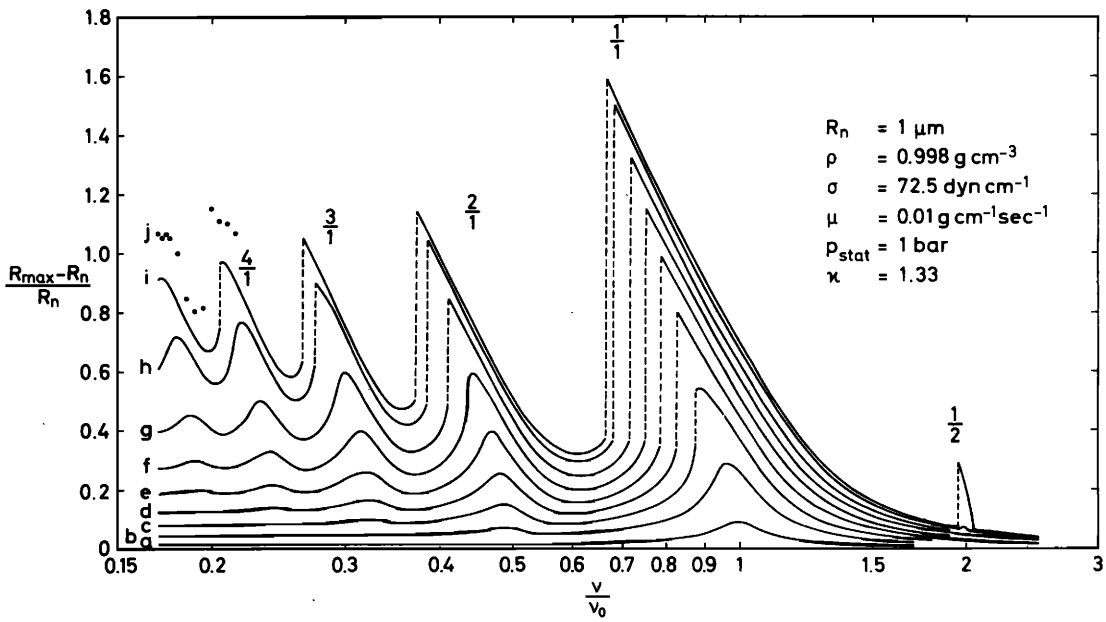

FIG. 4. Frequency response curves for a bubble in water with a radius at rest of $R_n = 1\ \mu m$ for different sound pressure amplitudes p_A of (a) 0.1, (b) 0.3, (c) 0.5, (d) 0.7, (e) 0.9, (f) 1.1, (g) 1.3, (h) 1.5, and (i) 1.6 bar. (j) Some points of the resonance curve for $p_A = 1.7$ bar (the first ultraharmonics occur).

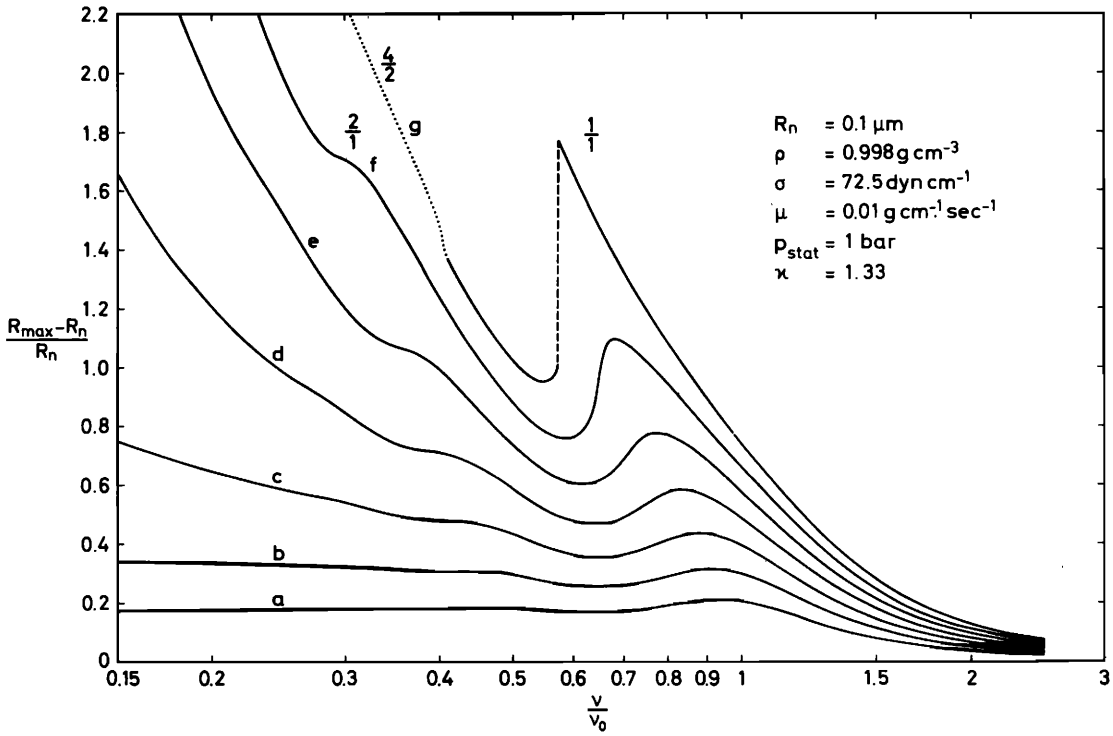

FIG. 5. Frequency response curves for a bubble in water with a radius at rest of $R_n = 1$ μm for different sound pressure amplitudes p_A of (a) 5, (b) 7, (c) 9, (d) 11, (e) 13, (f) 15, and (g) 17 bar.

Starting with the initial conditions of the steady state solution on the right-hand side of the jump a lower frequency was introduced into the equation and the new steady state solution calculated. This procedure simulates bubble response when the frequency is gradually lowered. The lowering of the frequency must be done in sufficiently small steps (in experiments sufficiently slow), otherwise the solution (bubble oscillation) will jump to the lower stable branch before being traced to its end. Figure 6 shows a hysteresis curve of this kind for a special case ($R_n = 1$ μm, $p_A = 0.7$ bar). The corresponding phase curve is given in Fig. 7. The phase relative to the phase of the driving sound pressure is plotted against the normalized frequency. A phase between 0° and 180° corresponds to tension [according to the sign of $p_A \sin\omega t$ in Eq. (3)], a phase between 180° and 360° to pressure on the bubble. Thus when the bubble is at its maximum at 90° it oscillates in phase with the sound field and at 270° out of phase. The behavior of the curves in Figs. 6 and 7 is well known from other nonlinear systems where the spring softens at higher amplitudes. A bubble behaves much like such a system because on the average the softening of the spring on elongation of the bubble overrides the hardening of the spring on compression.

The main resonance (like the others) broadens when

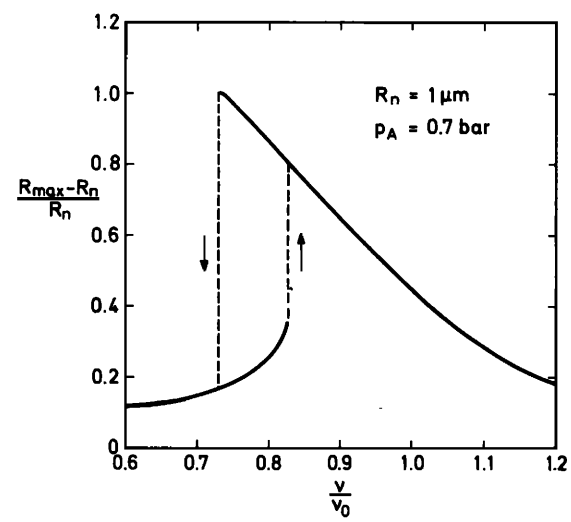

FIG. 6. The main resonance of a bubble in water with a radius at rest of $R_m = 1$ μm at a sound pressure amplitude of $p_A = 0.7$ bar showing the hysteresis phenomenon.

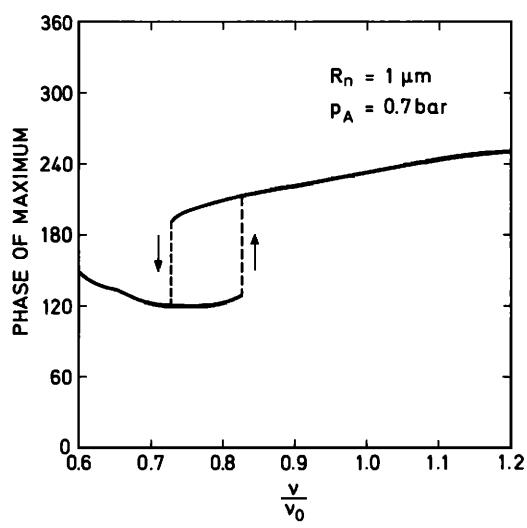

FIG. 7. Phase curve to Fig. 6.

the sound pressure amplitude p_A is raised. This must be attributed to the nonlinearity of the system. The broadening seems to have the effect that ultraharmonic resonances are swallowed before they have reached their threshold. This is supposed to be the case with the ultraharmonic of order $\frac{5}{4}$ at $R_n = 10$ μm (Fig. 3), while the ultraharmonic of order $\frac{4}{3}$ occurs just before being taken over. When looking at the Figs. 3–5 it seems as if it would be the fate of the ultraharmonics to be suppressed either by damping or by the other resonances at sufficiently high sound pressure amplitudes. But below we will see how they escape and even become predominating.

C. Harmonic resonances

The resonances in the vicinity of $\nu/\nu_0 = \frac{1}{2}, \frac{1}{3}, \frac{1}{4}, \ldots$ are the harmonics. They behave much like the main resonance, i.e., they lean over towards lower frequencies and show jump phenomena at sufficiently high pressure amplitudes. Their width is also growing with growing pressure amplitude leaving less space for the ultraharmonics. The harmonics are almost totally damped out at small bubble radii (Fig. 5, $R_n = 0.1$ μm) and for sufficiently small pressure amplitudes (Fig. 4, $R_n = 1$ μm). But the harmonics of higher order may grow faster with increasing sound pressure amplitude than the harmonics of lower order (Fig. 3, $R_n = 10$ μm). They at last always grow faster because at sufficiently high sound pressure amplitudes the amplitude of the bubble oscillation will grow with lowering of the frequency (see above).

When p_A is raised (near to p_B), new phenomena occur not observed with the main resonance.[20] It is the more or less gradual destruction of the harmonics because they apparently become unstable (or need special initial conditions). First the peaks of the harmonics will be taken over by ultraharmonics of order $\frac{4}{2}, \frac{6}{2}, \frac{8}{2}, \ldots$, or $\frac{6}{3}, \frac{9}{3}, \ldots$, or $\frac{8}{4}, \ldots$, instead of $\frac{2}{1}, \frac{3}{1}, \frac{4}{1}, \ldots$. No rules can be given which one of these ultraharmonics will occur first and at what location on the resonance. The situation indeed is very complex, and it turned out to

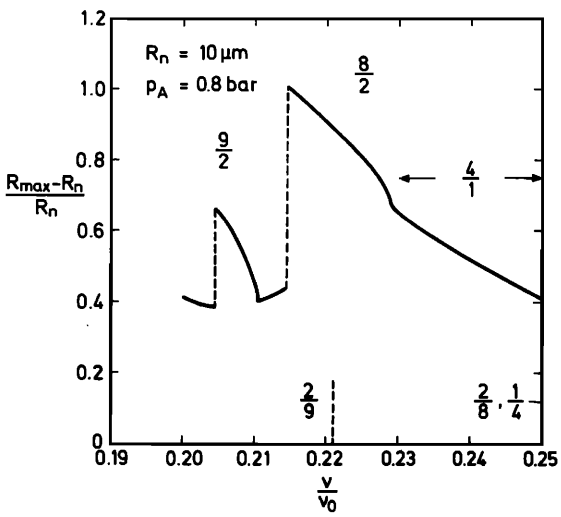

FIG. 8. The harmonic resonance of order $\frac{4}{1}$ and the ultraharmonics of order $\frac{8}{2}$ and $\frac{9}{2}$.

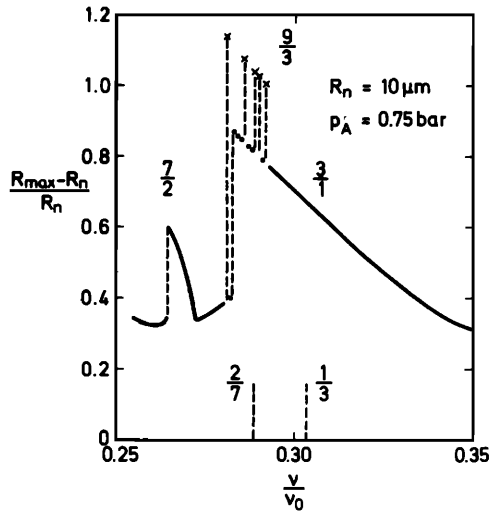

FIG. 9. The harmonic resonance of order $\frac{3}{1}$ and the ultraharmonics of order $\frac{8}{3}$ and $\frac{7}{2}$.

be impossible to calculate a nearly sufficient variety of what may happen. Only some examples can be given.

Figure 8 shows the region of the harmonic or order $\frac{4}{1}$ for a bubble with a radius at rest $R_n = 10$ μm and at a sound pressure amplitude $p_A = 0.8$ bar. Its peak has been taken over as a whole by the ultraharmonic of order $\frac{8}{2}$. Also shown is the ultraharmonic of order $\frac{9}{2}$ being shifted as a whole to lower frequencies.

Figure 9 shows another form of the destruction of a harmonic resonance ($R_n = 10$ μm, $p_A = 0.75$ bar, order $\frac{3}{1}$). A jumping occurs between the harmonic of order $\frac{3}{1}$ and a single ultraharmonic of order $\frac{8}{3}$. Because of the many jumps it is difficult to calculate the resonance curve adequately. Thus only some of the jumps are indicated by dashed lines. It should be noted that for getting a point of the resonance curve the initial condition always was a bubble at rest. This may be different to experimental situations, where perhaps the frequency is swept. Then other jumping effects are to be expected.

Jumps in the region of the harmonics may not only occur to an ultraharmonic of only one order, but resonances of many different orders may be involved. An example is given in Fig. 10 for the harmonic of order $\frac{2}{1}$ with the parameters $R_n = 10$ μm and $p_A = 0.8$ bar. In Fig. 10 all points calculated are plotted. A more detailed investigation was not done because of computer time considerations. Besides ordinary oscillations of order $\frac{2}{1}$ as in the case of lower pressure amplitudes, ultraharmonics of order $\frac{6}{3}$, one of $\frac{10}{6}$, and also some points of order $\frac{1}{1}$ were obtained. In the case of $\nu/\nu_0 = 0.41$ no steady-state solution could be obtained, but the oscillation amplitude was varying slightly around $(R_{max} - R_n)/R_n = 4.5$ (limits are given by the vertical bar) For a better visualization the points belonging to the same order of resonance are connected by dashed lines.

Even in the case where the harmonics are nearly totally damped out ($R_n = 0.1$ μm, Fig. 5), ultraharmonics were observed to occur in the region of the harmonics. The dotted part of the resonance curve at $p_A = 17$ bar in

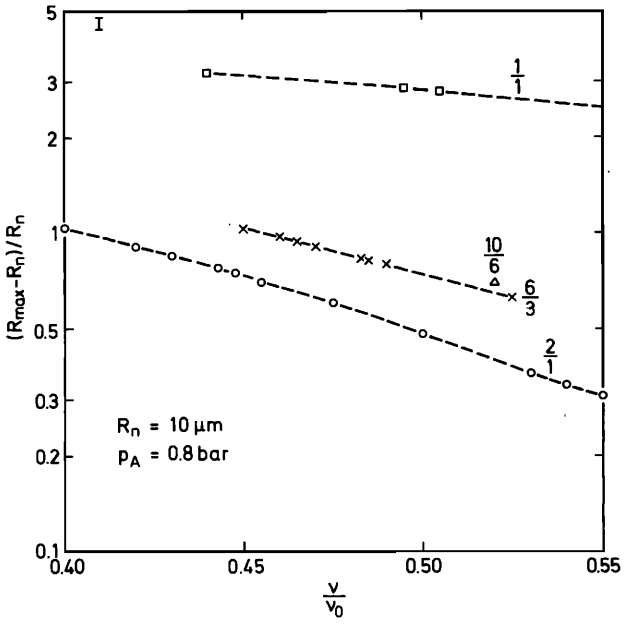

FIG. 10. Points of the resonance curve of a bubble in water with a radius at rest of $R_n = 10\ \mu m$ at a sound pressure amplitude of $p_A = 0.8$ bar in the region of the harmonic of order $\frac{2}{1}$. The different occurring resonances are indicated.

Fig. 5 is made up of an ultraharmonic of order $\frac{4}{2}$ gradually evolving from the curve (the harmonic of order $\frac{2}{1}$) at about $\nu/\nu_0 = 0.42$. This behavior is like that shown in Fig. 8 for a harmonic of order $\frac{4}{1}$ where the ultraharmonic of order $\frac{8}{2}$ gradually evolves from the harmonic.

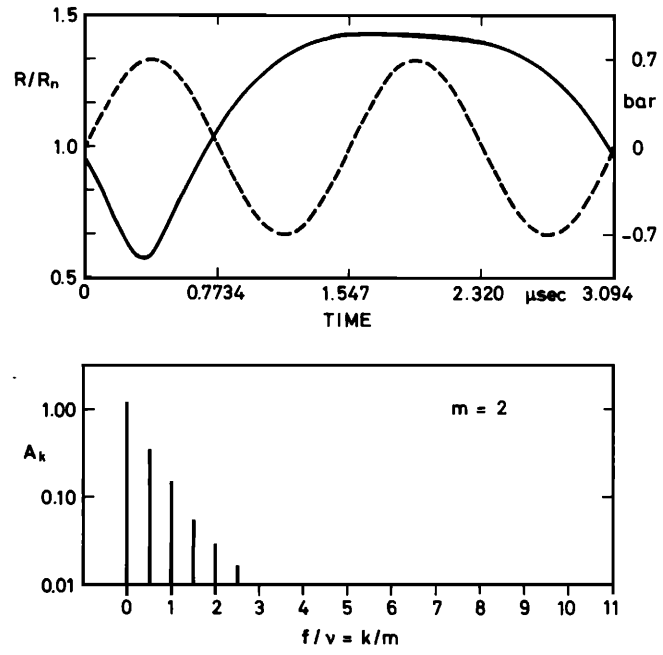

FIG. 11. Steady state oscillation (solid curve) of a bubble in water with a radius at rest of $R_n = 10\ \mu m$ at a sound pressure amplitude of $p_A = 0.7$ bar (driving pressure: dashed line) at a relative frequency of $\nu/\nu_0 = 1.95$. It is a subharmonic of order $\frac{1}{2}$. The first spectral components of this oscillation are shown in the lower part of the figure.

D. Subharmonic resonances

The resonances around $\nu/\nu_0 = 2, 3, 4, \ldots$ are the subharmonic resonances of order $\frac{1}{2}, \frac{1}{3}, \frac{1}{4}, \ldots$. The steady-state solutions have a least period of $2, 3, 4, \ldots$ periods of the driving sound field. An example of a subharmonic oscillation or order $\frac{1}{2}$ is given in Fig. 11 together with its spectrum. The spectrum (always) rapidly falls off, the frequency component at half the driving frequency being the strongest one. The same holds true for the subharmonic of order $\frac{1}{3}$, where the component at $\frac{1}{3}$ is the strongest one.

The subharmonic resonances lean over toward lower frequencies and show jumping phenomena like the main resonance and the harmonics (see Figs. 3–5). A new phenomenon with the subharmonics is that they have a threshold, i.e., a minimum sound pressure amplitude p_{At} before they set in. This onset is connected with a strong increase in amplitude.[14] Onset curves (maximum oscillation amplitudes in dependence on the sound pressure amplitude) are shown in Fig. 12 for the subharmonics of order $\frac{1}{2}$ at $\nu/\nu_0 = 2$ and of order $\frac{1}{3}$ at $\nu/\nu_0 = 3$ for a bubble of radius $R_n = 10\ \mu$m. The threshold for the onset of the subharmonics strongly depends on R_n and ν/ν_0. For a given bubble radius R_n the threshold has a minimum at very exactly $\nu/\nu_0 = 2, 3, 4$. It is believed that this is the case because the amplitudes of the oscillation at the onset are very small. Prosperetti[15] recently has given a formula for this threshold. For $\nu/\nu_0 = 2$ it is given by

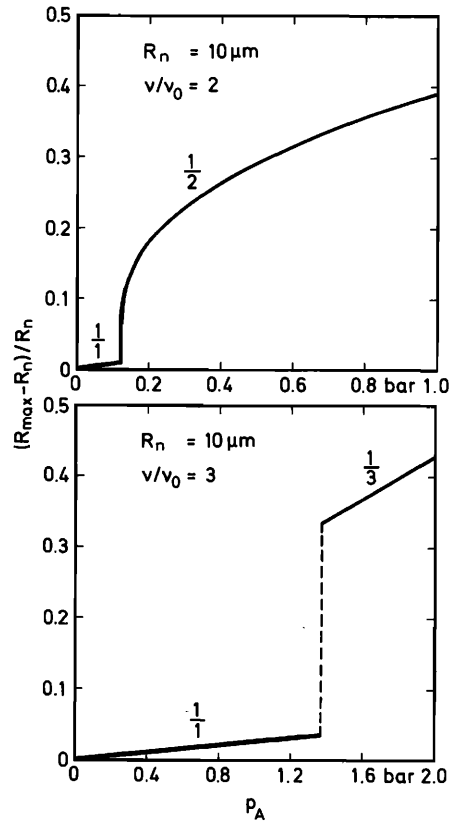

FIG. 12. Onset curves for a bubble in water with a radius at rest of $R_n = 10\ \mu$m at $\nu/\nu_0 = 2$ (upper diagram) and $\nu/\nu_0 = 3$ (lower diagram). Note the different scales for p_A.

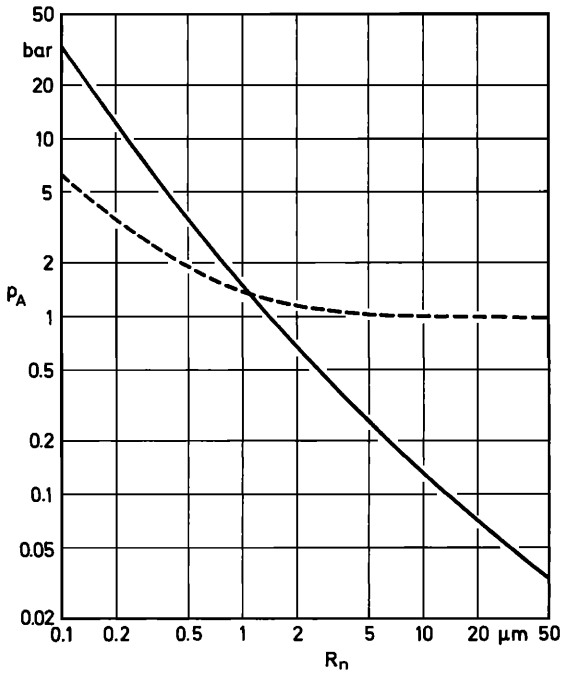

FIG. 13. Threshold for the occurrence of the first subharmonic oscillation (of order $\frac{1}{2}$ at $\nu/\nu_0=2$ in dependence on bubble radius (solid line) and Blake threshold (dashed line).

$$p_{At}=\frac{2\omega_0 b\, p_{stat}}{(1-w)\beta\left[1+\frac{16}{19}(b/\omega_0)^2\right]^{1/2}}\,, \tag{6}$$

with the abbreviations $\omega_0^2=3\kappa-w$, $w=2\sigma/R_n p_n$, $\beta=(9\kappa^2-w)/6\omega_0^2$, and $b=2\mu/R_n(p_n\rho)^{1/2}$. This threshold agrees very well with numerical calculations. This again is believed to be the case because the oscillation amplitudes at the onset are very small. Figure 13 shows the threshold curve $\nu/\nu_0=2$ in dependence on R_n (solid line) as numerically calculated. The curve of Eq. (6) fits this curve within the thickness of the line. To have an idea of the magnitude of the threshold value the Blake threshold [Eq. (5), see above] is also plotted in Fig. 13 (dashed line). The curves cross each other at about $R_n=1\mu$m. For smaller radii the threshold value for the onset of the first subharmonic quickly becomes considerably higher than the Blake threshold. This comparison is interesting insofar, as it is known from the resonance curves (Figs. 3–5) that in the vicinity of the Blake thresholds the bubble oscillation will become extremely heavy (for not too high driving frequencies).

The threshold curve of Fig. 13 can be transformed into a threshold curve in dependence on the driving frequency (Fig. 14). As a comparison with the experimentally obtained thresholds for the onset of cavitation of Esche[5] shows, the values are much lower indicating that viscosity will only be of minor influence in determining the cavitation threshold of water.

So far we had a closer look at the subharmonic oscillations at $\nu/\nu_0=2$. As we see from Fig. 3 the subharmonic resonances expand in area with increasing sound pressure amplitude like the other resonances. Thus they occur in an increasing region around $\nu/\nu_0=2$ (and $3,4,\ldots$). In Fig. 15 the threshold curve for the onset of a subharmonic oscillation of a bubble with a radius of $R_n=10$ μm is given for $1.6\leq\nu/\nu_0\leq3.4$. Below this curve the bubble oscillates with the period of the driving sound field, above this curve, but only very near to this curve, subharmonically with the order indicated ($\frac{1}{2}, \frac{2}{5}, \frac{1}{3}$). The region above the threshold curve was not investigated. It will show a very complicated topology as various ultraharmonics will occur that are not at all predictable.

When curves like that of Fig. 15 are calculated for other bubble radii it turns out that they may look totally different. For instance, the threshold for the occurrence of the first subharmonic (of order $\frac{1}{2}$) may be lower even at $\nu/\nu_0=3$. In Fig. 16 the maximum amplitude

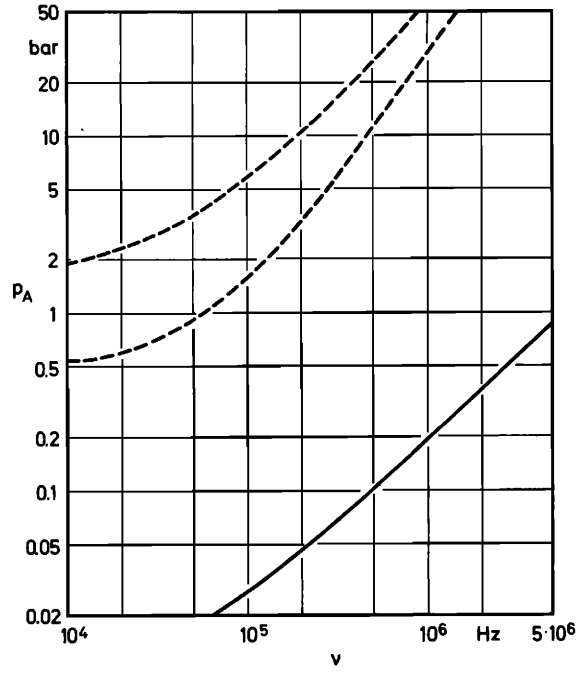

FIG. 14. Threshold for the occurrence of the first subharmonic oscillation at $\nu/\nu_0=2$ in dependence on the frequency (solid line). The dashed lines are the experimentally found limiting curves of Esche[5] for the onset of cavitation.

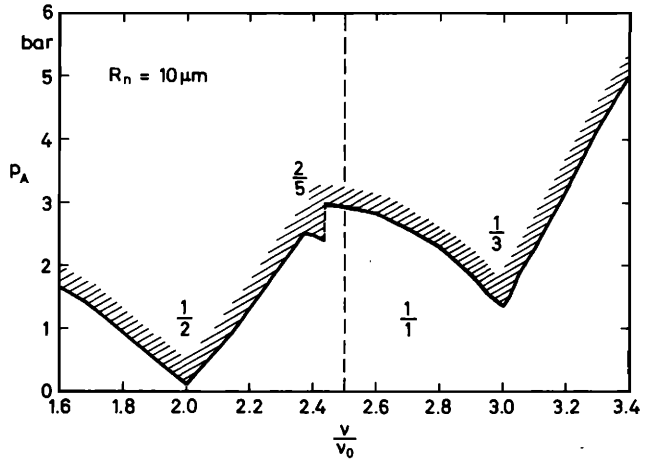

FIG. 15. Threshold curve for the onset of subharmonics or ultraharmonics for a gas bubble in water with a radius at rest of $R_n=10$ μm. The numbers indicate the order of the resonance.

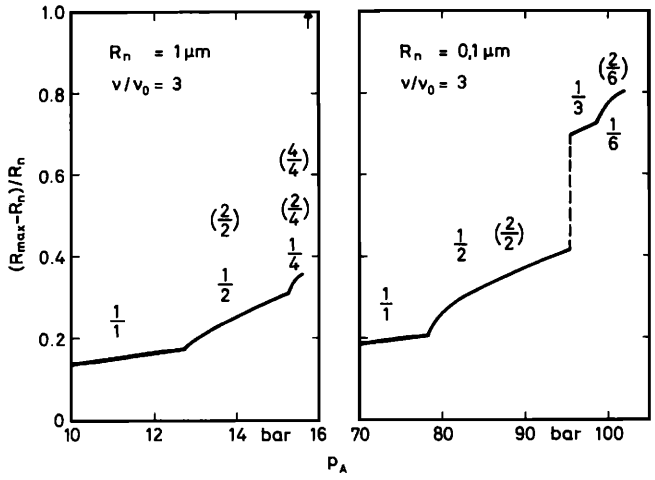

FIG. 16. Onset curves at $\nu/\nu_0 = 3$ for two bubbles with radii of $R_n = 1$ and 0.1 μm. The numbers indicate the order of the subharmonic (or ultraharmonic) resonance (compare Fig. 12).

of the oscillation at $\nu/\nu_0 = 3$ is shown in dependence on the sound pressure amplitude p_A for two bubble radii ($R_n = 1$ and 0.1 μm). They are quite different from the onset curve for $R_n = 10$ μm (Fig. 12). In the case of $R_n = 0.1$ μm prior to the onset of the subharmonic of order $\frac{1}{3}$, the subharmonic of order $\frac{1}{2}$ occurs which perhaps better may be said to be of order $\frac{2}{2}$. (As noted in the Introduction, the ultraharmonics are in some cases different to classify). The subharmonic of order $\frac{1}{3}$ soon changes into one of order $\frac{1}{6}$ or $\frac{2}{6}$. Even more complicated is the case for $R_n = 1$ μm. First the subharmonic of order $\frac{1}{2}$ or $\frac{2}{2}$ appears, then that of order $\frac{1}{4}$ (or $\frac{2}{4}, \frac{4}{4}$). For $p_A = 15.7$ bar and some higher values tried no steady-state solutions could be reached even after relatively long computation.[21] Thus the oscillation of order $\frac{1}{3}$ could not be found. It seems to be shifted totally away from $\nu/\nu_0 = 3$.

E. Ultraharmonic resonances

An example of an ultraharmonic oscillation of order $\frac{5}{2}$ has already been given in Fig. 2. Whole resonance curves are to be seen in Fig. 3 (set of resonance curves for $R_n = 10$ μm) and in Figs. 8 and 9. They lean over towards lower frequencies like the other resonances, have thresholds for their occurrence like the subharmonics and usually are shifted totally towards lower frequencies. As an example the ultraharmonic of order $\frac{9}{2}$ in Fig. 8 may be considered. At the location of $\nu/\nu_0 = \frac{2}{9}$ the resonance $\frac{8}{2}$ occurs. Thus the ultraharmonics often may be found only by carefully looking for them, especially near the threshold where the region of ν/ν_0 for ultraharmonic oscillations goes to zero.

In close connection with this shifting another feature of subharmonics is observed. At given R_n and ν/ν_0 an ultraharmonic may return with increasing sound pressure amplitude p_A to an oscillation with the period of the driving sound field. This can be seen from Fig. 17, where three ultraharmonics of order $\frac{3}{2}$ are given for a bubble of radius $R_n = 10$ μm for $p_A = 0.5$, 0.6, and 0.7 bar. The resonance gets broader with increasing sound pressure amplitude, but at the same time it is shifted such an amount towards lower frequencies that the curves intersect. Thus when the sound pressure amplitude is increased at constant frequency the ultraharmonic will set in and set out again.

It is believed that at sufficiently high sound pressure amplitudes only ultraharmonic oscillations will be stable (in case stable oscillations exist at all). In connection with the harmonics at higher sound pressure amplitudes we have already discussed, how ultraharmonics may intrude into their domain and become predominant. The details are very complex, and it was not found worthwhile to study them beyond the data given in Figs. 8–10.

III. DISCUSSION

Forced oscillations of gas bubbles in liquid have been investigated numerically using a special bubble model. The investigation is done on a totally numerical basis. The deficiency of numerical investigations that only a limited number of parameter sets can be investigated was partly overcome by a big input of computer time. Another deficiency of numerical investigations is that much space is needed to present the results. It was therefore tried to classify the results and to describe only the most essential features detected.

A. Features of bubble resonances

(1) A bubble may be driven to high amplitudes in its oscillation at driving frequencies ν being close to a rational number m/n ($m, n = 1, 2, 3, \ldots$) times the linear resonance frequency ν_0 of the bubble. Only the resonances, where m and n are small natural numbers are observed up to fairly high pressure amplitudes (see Figs. 3–5). The resonances are classified according to their "order" being the inverse of m/n.

(2) All resonances lean over towards lower frequencies and eventually show jump phenomena depending on the direction of the frequency alteration (Figs. 6 and 7).

(3) Subharmonic and ultraharmonic oscillations only

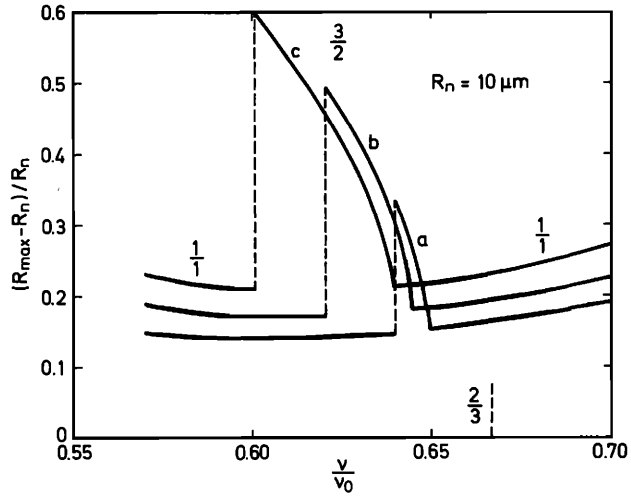

FIG. 17. The ultraharmonic of order $\frac{3}{2}$ for a bubble in water with a radius at rest of $R_n = 10$ μm at sound pressure amplitudes p_A of (a) 0.5, (b) 0.6, and (c) 0.7 bar. The numbers above the curves indicate the order of the oscillation.

occur beyond some threshold value of the driving sound pressure amplitude. The analytic formula given by Prosperetti[15] [this paper is Eq. (6)] for the first subharmonic at $\nu/\nu_0 = 2$ agrees very well with the numerical calculation.

(4) The ultraharmonic resonances (as far as they occur at all) are shifted as a whole towards lower frequencies from their position they would have at small amplitudes [i.e., an ultraharmonic of order n/m may be found at driving frequencies below $\nu = (m/n)\nu_0$]. This simply may be explained by the fact that they set in at rather high oscillation amplitudes where ν_0 must be replaced by some value ν_f of the free oscillation corresponding to some mean amplitude value of the steady state oscillation.

(5) When the sound pressure amplitude is raised from low values the resonance curve as a whole will totally alter its appearance.

(5.1) Big bubbles ($R_n = 10$ μm, Fig. 3) will show many pronounced peaks at the location of the harmonics, subharmonics, and (somewhat shifted) ultraharmonics. The higher harmonics ultimately grow faster than the lower harmonics and so do the higher ultraharmonics. At some value of the sound pressure amplitude (below the Blake threshold of $p_B = 0.997$ bar), the ultraharmonics start to take over the harmonics (Figs. 8–10). At still higher sound pressure amplitudes, being near the Blake threshold, the normal appearance of the frequency response curve is lost by the many jumps between the branches of the many possible resonances (like in Fig. 10). Also very heavy oscillations occur with amplitudes and collapses far beyond the validity of the bubble model used.

(5.2) The resonance curve for a bubble with a radius at rest of $R_n = 1$ μm (Fig. 4) look only somewhat different in that higher pressure amplitudes are needed to excite the bubble and that the ultraharmonics have a high threshold. They indeed only set in above the Blake threshold of $p_B = 1.408$ bar (in the frequency range considered) and first (within the pressure amplitude step size) occur in the peaks of the harmonics (see Fig. 4, $p_A = 1.7$ bar, the dots).

(5.3) The resonance curves for a bubble with a radius at rest of $R_n = 0.1$ μm (Fig. 5) look quite different. All resonances are almost damped out. The main resonance becomes appreciable only for high sound pressure amplitudes (far above the Blake threshold of $p_B = 6.379$ bar). The curves can easily be calculated even for values far above the Blake threshold as jumping phenomena do not occur. Above the Blake threshold the curves seem to grow on an exponential scale with decreasing frequency. Ultraharmonics are observed in this case of a heavily damped bubble, too. The dotted part of the curve g of Fig. 5 ($p_A = 17$ bar) is the ultraharmonic of order $\frac{4}{2}$.

B. On the connection of ultraharmonics and the first subharmonic in the spectrum of cavitation noise

Some inferences can already be made from the occurrence of the ultraharmonics of order $n/2$ below the main resonance on the occurrence of the first subharmonic (one half the driving frequency) in the spectrum of the cavitation noise. The first explanation was proposed by Güth[4] who attributed this spectral line at half the driving frequency to the first subharmonic oscillation at $\nu/\nu_0 = 2$. Thus the liquid must contain bubbles being driven at twice their resonance frequency. This conflicts with the observation that only bubbles smaller than resonant size are present in the liquid.[22] In view of the results presented here, the first subharmonic (of order $\frac{1}{2}$, occurring near $\nu = 2\ \nu_0$) do not need to be involved. Indeed, ultraharmonics of different kinds (of order $n/2$, $n = 2, 3, 4, \ldots$, or $n/4, \ldots$) are encountered below the main resonance that shows a component at half the driving frequency in their spectrum of the bubble wall motion. It is proposed that these (of course only some of these) are the source of the first subharmonic in the spectrum of the cavitation noise.

As the onset of the first subharmonic in the spectrum of the cavitation noise has been proposed as a method to determine the cavitation threshold (indeed it is in itself a special sort of cavitation threshold), the question arises which ultraharmonic (of which order) below the main resonance will have the lowest threshold. This can be calculated in principle, but has not yet been done, because the ultraharmonics are difficult to locate (in ν and p_A) especially at their onset. In practical situations, in addition, the subharmonic threshold will depend in a complicated way on the bubble size spectrum. For big bubbles ($R_n > 10$ μm) it can be predicted that the ultraharmonic of order $\frac{3}{2}$ has the lowest threshold. It has been calculated in dependence on the frequency ν of the sound field for $R_n = 10$ μm and displays interesting features analogous to those observed by Barger[23] in his cavitation threshold measurements. From space considerations details will be given elsewhere. For bubbles smaller than about 10 μm nothing can be said definitely. It may be that many ultraharmonics may set in almost simultaneously (see Fig. 4, the points) or that the first occurrence is shifted to very far below the main resonance, as it is expected for $R_n = 0.1$ μm (Fig. 5). In Fig. 5 the bubble of curve (b) ($p_A = 7$ bar) is already driven above the Blake threshold, and its amplitude grows with decreasing frequency. It can be expected that at high amplitudes of the oscillation ultraharmonics will set in at low frequencies.

This complicated situation shows that despite of its experimental suitability as a measure of some sort of cavitation threshold the first subharmonic in the spectrum of the cavitation noise is not easily related to bubble dynamics. Experiments are under way to gain more insight into the relationship by sophisticated spectral measurements. Recent measurements done in our laboratory by Heinrich[24] indicate that indeed ultraharmonic bubble oscillations may be the source of the first subharmonic noise component, as the spectral lines at $\frac{3}{2}\nu$ (ν the driving sound frequency) and $\frac{5}{2}\nu$ appear at lower pressure amplitudes than the subharmonic spectral line at $\frac{1}{2}\nu$. This strongly supports the suggestions of the role of the ultraharmonic bubble oscillations stated above and arrived at before the measurements were done.

ACKNOWLEDGMENTS

This work has only become possible through the use of many digital computers (IBM 7040, IBM 7090, Univac 1108, Honeywell H 632). Most of the calculations were done using the Univac 1108 of the Gesellschaft für Wissenschaftliche Datenverarbeitung, Göttingen, West Germany. For convenience the plotting of the steady-state oscillations and the spectrum of the bubble wall motion was done on the Honeywell H 632 of the Third Physical Institute of the University of Göttingen. This computer has been granted by the Stiftung Volkswagenwerk. Also, I want to express my thanks to A. Prosperetti for making available to me his formula for the threshold of the first subharmonic oscillation prior to publication.

*This work was sponsored by the Fraunhofer–Gesellschaft.

[1]H. G. Flynn, "Physics of Acoustic Cavitation in Liquids," in *Physical Acoustics*, edited by W. P. Mason (Academic, New York, 1964), Vol. IB, pp. 57–172.

[2]R. T. Knapp, J. W. Daily, and F. G. Hammitt, *Cavitation* (McGraw–Hill, New York, 1970).

[3]*High-Intensity Ultrasonic Fields*, edited by L. D. Rozenberg, (Plenum, New York, 1971).

[4]W. Güth, Acustica **6**, 532–538 (1956).

[5]R. Esche, Acustica **2**, AB 208–AB 218 (1952).

[6]E. A, Neppiras and J. Parrott, Proceedings of the 5th International Congress on Acoustics, Liege, 1965, paper D51.

[7]P. DeSantis, D. Sette, and F. Wanderlingh, J. Acoust. Soc. Am. **42**, 514–516 (1967).
(1968).

[8]E. A. Neppiras, IEEE Trans. Sonics Ultrason. **15**, 81–88

[9]P. W. Vaughan, J. Sound Vib. **7**, 236–246 (1968).

[10]E. A. Neppiras, J. Acoust. Soc. Am. **46**, 587–601 (1969); J. Sound Vib. **10**, 176–186 (1969).

[11]A. Eller and H. G. Flynn, J. Acoust. Soc. Am. **46**, 722–727 (1969).

[12]A. Mosse and R. D. Finch, J. Acoust. Soc. Am. **49**, 156–165 (1971).

[13]E. A. Neppiras and R. D. Finch, J. Acoust. Soc. Am. **52**, 335–343 (1972).

[14]W. Lauterborn, Acustica **20**, 370–371 (1968); Acustica **22**, 238–239 (1969/70); Acustica **23**, 73–81 (1970); Proc. 7th Int. Congr. Acoust., Budapest, paper 20 U15, **4**, 477–480 (1971).

[15]A. Prosperetti, J. Acoust. Soc. Am. **56**, 878–885 (1974).

[16]Lord Rayleigh, Philos. Mag. Ser. 6, **34**, 94–98 (1917).

[17]M. S. Plesset, J. Appl. Mech. **16**, 277–282 (1949).

[18]B. E. Noltingk and E. A. Neppiras, Proc. Phys. Soc. Lond. B**63**, 674–685 (1950); B**64**, 1032–1038 (1951).

[19]H. Poritsky, "The Collapse or Growth of a Spherical Bubble or Cavity in a Viscous Fluid," in *Proceedings of the First U. S. National Congress on Applied Mechanics*, edited by E. Sternberg (New York, 1952), pp. 813–821.

[20]It is believed that similar phenomena will occur with the main resonance, but only at very high-pressure amplitudes. The oscillation will then be very heavy, and shape stability questions will become important.

[21]20–30 min on a Univac 1108.

[22]High-speed photography and holography were applied to look for bubbles double the resonant size in a cavitation bubble field produced ultrasonically. In no case such a bubble showed up.

[23]J. E. Barger, Thresholds of Acoustic Cavitation, Tech. Mem. No. 57, Acoust. Res. Lab., Harvard U., Cambridge, MA (1964).

[24]G. Heinrich, Ph. D. thesis (Göttingen, 1974).